Conducting and stretchable nanometer-thin gold/thiol-functionalized polydimethylsiloxane films

Bekim Osmani
Tino Töpper
Bert Müller

Conducting and stretchable nanometer-thin gold/thiol-functionalized polydimethylsiloxane films

Bekim Osmani, Tino Töpper, and Bert Müller*

University of Basel, Biomaterials Science Center, Department of Biomedical Engineering, Allschwil, Switzerland

Abstract. Future low-voltage dielectric elastomer transducers (DETs), based on nanometer-thin elastomer membranes, will rely on soft and compliant electrodes with reasonable electrical conductivity and sound adhesion to the elastomer. State-of-the-art adhesion promoters, including nanometer-thin Cr/Ti films, result in defects for applied areal strains larger than 3% and lead to increases in the stiffness of DETs. To generate forces in the Newton range, these low-voltage DETs have to be stacked in thousands of layers. Herein, we present a compliant electrode, which consists of gold bonded covalently to thiol-functionalized polydimethylsiloxane (SH-PDMS) films. The membranes were fabricated using molecular beam deposition and *in situ* and/or subsequent ultraviolet light (UV) radiation. Peel-off tests demonstrate the expected strong binding of Au to the SH-PDMS network, with this highly stretchable Au/SH-PDMS layer capable of withstanding strains of at least 60%, without losing conductivity. Optical micrographs show signs of cracks for strained pure Au and Au/Cr electrodes but not for the Au/SH-PDMS layer. The mechanical properties and adhesion forces of Au/SH-PDMS were extracted by means of atomic force microscopy (AFM), using a spherical Au tip coated with methyl groups (CH_3). The elastic modulus of (12 ± 9) MPa increased slightly against the 20-nm-thin Au/PDMS example, but it can be tailored by the cross-linking density of Au/SH-PDMS via the UV irradiation dose. Unloading nanoindentation curves revealed pull-off forces between the CH_3-functionalized AFM tip and the Au/SH-PDMS layer at the time of separation. For Au/SH-PDMS, the spectral distribution of pull-off forces exhibits repulsive forces with the CH_3 groups of the PDMS network as well as adhesive forces resulting from interactions with the nanometer-sized Au clusters. This approach provides the means to bind gold clusters homogenously within the SH-PDMS film. Such compliant electrodes are the prerequisite for fabricating low-voltage DETs that can be stretched by more than 50%. © *The Authors. Published by SPIE under a Creative Commons Attribution 3.0 Unported License. Distribution or reproduction of this work in whole or in part requires full attribution of the original publication, including its DOI.* [DOI: 10.1117/1.JNP.12.033006]

1 Introduction

Dielectric elastomer transducers (DETs) are smart devices as they can operate as a sensor, an actuator, an electric energy harvester, and a self-sensing actuator.[1–4] State-of-the-art DETs are based on elastomer membranes with micrometer thickness and are often fabricated by spin-coating, doctor-blading, or PAD-printing.[5,6] These DETs need to be operated at hundreds of volts to reach strains above 20%.[7,8] Recently, 200-nm-thin DETs have been manufactured using molecular beam deposition and operated at 12 V.[9]

Nanometer-thin DETs are well suited for sensing, but to provide the forces of fecal sphincters, they have to be stacked.[10,11] The generated force scales with the active area and therefore

---

*Address all correspondence to: Bert Müller, E-mail: bert.mueller@unibas.ch

with the number of layers in the stacked DET. For such low-voltage DETs, nanometer-thin, compliant electrodes are a prerequisite. Conventional metal films, however, dominate the mechanical properties of the stack and prevent the desired DET operation.[12] Currently, the electrodes are based not only on metallic thin films but also on carbon powder or nanotubes, or the implantation of metallic nanometer-sized clusters into the elastomer membrane.

Metal films, including Au, have been deposited on elastomer membranes using various cathodic sputtering, electron beam, and thermal evaporation techniques.[13] Such conductive layers have obtained the clearance of the Food and Drug Administration (FDA) for a variety of medical implants, but they still involve a number of major challenges.

First, pure metals and metallic alloys exhibit a Young's modulus that exceeds those of currently used elastomers by significant orders of magnitude;[14] for example, the elastic modulus of Au corresponds to 79 GPa, whereas for sandwiched elastomer membranes, it is often below 1 MPa.[14] Even Au layers as thin as 15 nm increase DET stiffness by about one order of magnitude; consequently, bright ideas have to be developed to limit the mechanical impact of the conductive layer on the overall DET-stack. One recently presented method takes advantage of metal films under compressive stress as seen in wrinkled metal films on polymers.[15] This apparent stiffness reduction works well for strain values below 20%, and it is advantageous not only for stacked DETs, but also for many other applications, including mechanically adapted computer–brain interfaces for stimulation and read-out.[16]

Second, the elasticity of pure metals and metallic alloys, even in films as thin as 20 nm, is generally limited to a maximal 3%, before cracks form.[17] These defects significantly reduce the layer's conductivity; nevertheless, layers of 2-nm Cr and 50-nm Au, prepared on elastomeric substrates, withstand uniaxial strains of 20%, without loss of conduction. During operation, a network of cracks and metal islands in the individual metal films develops, which probably is hardly controlled in the multistack configuration.

Third, the adhesion of metals to polymers can be insufficient. For example, Au delaminates from polydimethylsiloxane (PDMS), which is bypassed by introducing Cr or Ti layers.[18] Such additional metal films, however, lead to a substantial increase in the DET's stiffness. Furthermore, it alters the planar topology of the elastomer membrane by wrinkle formation. Alternatively, one can achieve the necessary adhesion between Au and PDMS by incorporating a molecular adhesive, such as (3-mercaptopropyl)trimethoxysilane (MPTMS).[19] This methodology, however, requires silanol functional groups on the PDMS surface to be achievable via oxygen plasma and ultraviolet/ozone treatments.[20–22] These treatments evoke a silica-like surface layer, which gives rise to cracks for strains above 10%.

Fourth, metallic species frequently diffuse into the polymer membranes, a phenomenon generally found for Au in pure PDMS. As a final result, the nanometer-thin metal film vanishes and its parts migrate through the elastomer membrane in an uncontrolled manner. A diffusion of Au into the PDMS network may be reduced by incorporating thiol groups into the polymer chains, as thiols and disulfide bonds interact strongly with Au.[23,24]

In the present communication, we show that all the challenges listed above can be mastered for the Au-PDMS system by incorporating a nanometer-thin thiol-functionalized PDMS interlayer. In this manner, the Au-based 85-nm-thin compliant electrode forms no cracks for strains as large as 60%, acts as a diffusion barrier and remains highly conductive.

2 Experimental

2.1 Molecular Beam Deposition of Nanometer-Thin Elastomer Films

Supplied materials were evaporated thermally under ultrahigh vacuum (UHV) conditions at a base pressure of 10^{-7} mbar. Synthesized thiol-terminated polydimethylsiloxane (SH-PDMS) was evaporated using low-temperature effusion cells (NTEZ, Dr. Eberl MBE Komponenten GmbH, Weil der Stadt, Germany) with a 2 cm^3 crucible. The material was evaporated at a crucible temperature of 140℃, well below the thermal degradation temperature of vinyl and thiol end groups[22,25] and corresponding to a deposition rate of about 30 nm h^{-1}.

Stretchable substrates of 1-mm thick were prepared by casting PDMS (Dow Corning, Sylgard® 184 and OS-20 Fluid, Dow Corning Europe SA, Belgium) at a ratio of 10:1:10

of elastomer to curing agent to solvent on polystyrene films. Subsequently, the PDMS substrates were cured thermally at a temperature of 70°C for a duration of 24 h. These membranes were stabilized during the deposition by mounting them to a Si-substrate (Siegert Wafers GmbH, Germany) at a distance of 450 mm from the crucibles and the UV lamp. UV cross linking of the SH-PDMS was initiated *in situ* and/or by subsequent irradiation from an externally mounted source (H_2D_2 light source L11798, Hamamatsu, Japan) through a CaF_2-window.[9] The spectrum of the deuterium UV lamp ranged from 160 to 450 nm, with a peak intensity at a wavelength of ~190 nm. At irradiation wavelengths below 190 nm, methyl groups become sensitive to radicalization, so C—H or even Si—C bonds are radicalized and methyl side groups are separated from the Si-O backbone of the PDMS chain.[9,26,27]

The growth of the metal and elastomer films was controlled using the spectroscopic ellipsometer SE801 (Sentech Instruments GmbH, Berlin, Germany) and cross checked via atomic force microscopy surface scans along intentionally induced scratches. To examine *in situ* the optical properties of the forming nanostructures, SpectraRay3 software was utilized. Spectroscopic Ψ- and Δ-values in the range 190 to 1050 nm were monitored at a frequency between 0.5 and 2 Hz at an incident angle of 70 deg to the normal of the substrate surface. The 4-mm-wide incident beam resulted in a 4×10 mm^2 spot area on the substrate.

For comparison, dimethyl silicone copolymer films containing thiol (—SH) side groups with an average molecular weight of 3600 g/mol (GP-367, Genesee Polymers Corporation) were prepared by spin-coating at a speed of 6000 rpm for a period of 2 min. The films were UV-cured for a period of 10 min with a 200 W Hg Xe UV lamp (super-quiet mercury-xenon lamp L2423, Hamamatsu Photonics K.K., Hamamatsu, Japan) at a distance of 500 mm.

2.2 *Thermal Evaporation of Gold and Chromium*

To prepare the electrodes, gold and chromium were evaporated thermally in the UHV system at a residual pressure of 10^{-7} mbar. Two high-temperature effusion cells (HTEZ, Dr. Eberl MBE Komponenten GmbH, Weil der Stadt, Germany) with 10-cm^3 PBN crucibles served as molecular beam sources. The evaporation temperatures for gold and chromium were set at 1400°C and 1440°C, corresponding to a deposition rate of about 1.1 and 0.3×10^{-2} nm s^{-1}, respectively. The substrate was mounted at a distance of 450 mm from the crucibles.

2.3 *Atomic Force Microscopy Imaging*

The topology of the electrodes was determined by raster-scanning spots of 20×20 μm^2 with a soft atomic force microscopy (AFM) probe (Tap190Al-G probe, NanoAndMore GmbH, Wetzlar, Germany) in a tapping mode (vibration amplitude of 420 nm, set point 70%), using a FlexAFM System (Nanosurf AG, Liestal, Switzerland). For each image, 512 lines were acquired at a speed of one line per second. The raw data were leveled by subtracting a mean plane and removing a polynomial background of second degree. Root mean square (RMS) roughness values were calculated using the open-source software for SPM data analysis Gwyddion, Version 2.41.

2.4 *Peel-Off Tests and Electrical Conductivity*

Peel-off tests were performed using transparent tape (3M, Scotch® Transparent Tape Dispensered Roll, 3M Europe SA). The tape was first laid on the electrode and gently pressed to establish a uniform contact. In a second step, the tape was peeled-off manually at an angle of 90 deg from the substrate. The results are rated in a qualitative manner. We then determined whether the electrode remained on PDMS film or were transferred to the adhesive tape.

To get an idea on the conductivity of the Au-based film under strain, resistance was determined as the function of the applied strain with a simple instrument (Multimeter Fluke 23 Series II). The instrument compares the resistance of Au-based films with an internal reference. The wiring was achieved using GaIn metal drops. The liquid contacts exhibited a distance of 10 mm at zero strain.
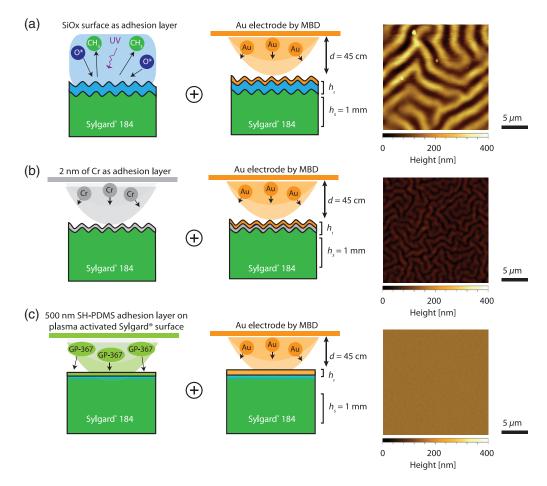
2.5 *Elastic Modulus and Pull-Off Forces*

The elastic modulus E_f and the adhesion forces at separation, termed "pull-off forces," were derived from AFM-based nanoindentation experiments. Each area of interest was partitioned into 1600 domains, which serve as nanoindentation sites. For each nanoindentation site, the Johnson–Kendall–Roberts (JKR) contact model, taking into account adhesion forces between the cantilever tip and the electrode surface, was fitted along the entire backward indentation curve. AFM indentations (FlexAFM C3000, Nanosurf AG, Switzerland) were applied on $40 \times 40~\mu m^2$ spots using a cantilever with a colloidal particle with a radius of $(1.0 \pm 0.2)~\mu m$ (CP-FM-Au-A, sQUBE, NanoAndMore GmbH, Germany). The spring constant $k = (2.4 \pm 0.1)$ nm of the AFM cantilever was determined using the Sader method.[28] The elastic modulus for each domain was calculated from the force–distance curves. It has been reported that indentation measurements using large spheres on soft polymers are affected significantly by adhesion forces F_{adh}.[29] The JKR model was implemented in FLEXANA® software (FLEXANA, Nanosurf AG, Switzerland), offering a fully automated postprocessing and analysis of the data.[29]

3 Results and Discussion

3.1 *Comparison of Adhesion Promoters*

The low adhesion of gold to commercially available Sylgard® 184-PDMS is well documented.[30] In Fig. 1, we compare state-of-the art adhesion techniques with the proposed approach using

Fig. 1 Comparison of adhesion promotors for gold films on Sylgard® substrates. AFM surface scans are presented for gold films on (a) oxygen plasma-treated PDMS, on (b) 2-nm Cr layers, and (c) a 500 nm-thin spin-coated SH-PDMS film.

thiol-functionalized PDMS. The peel-off test clearly demonstrates that gold could be removed partially from oxygen plasma-treated polymer and from the polymer covered by 2-nm Cr. As one can see in parts (a) and (b) of Fig. 1, the surface forms wrinkles. The adhesion layers, given a blue color for the plasma treatment and a gray color for the Cr, have a thermal expansion coefficient that differs from the underlying bulk PDMS. Films deposited at source temperatures above 1400°C form wrinkles in the course of cooling down to room temperature.
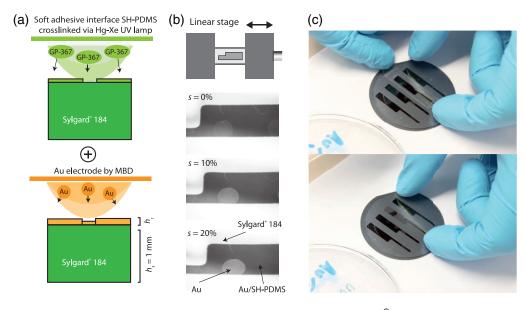
In addition to these wrinkles, cracks occur to release compressive stress. The peak-to-peak amplitude of the gold on the plasma-treated PDMS films was (300 ± 100) nm, whereas the 2-nm Cr induced a mean amplitude of (140 ± 20) nm. These large values indicate that only the gold on the protrusions had been removed by the peel-off tests. The AFM study supports this assumption because we observed a phase shift of (70 ± 20) deg when scanning from the protrusion to the depletion.

The deposition of SH-PDMS as an adhesion interface, and the subsequent thermal evaporation of gold, led to a flat surface—as verified by AFM images exemplified in Fig. 1(c). The peel-off tests, however, showed that the Au/SH-PDMS double layer on native PDMS could be removed, too. The bonding between the Au/SH-PDMS and the Sylgard® PDMS substrate is obviously weak. To validate this assumption, we fabricated Au/SH-PDMS electrodes on a Si wafer with a native 3-nm-thin oxide. In this case, the Au/SH-PDMS could not be peeled-off and remained fully intact.

Fabricated as submicrometer films, SH-PDMS tends to form extended characteristic defects on native Sylgard® PDMS, as shown in Fig. 2. Due to the repelling interactions of the methyl groups at the substrate and SH-PDMS, round-shaped defects were observed, cf. Fig. 2(b). Gold deposited on native Sylgard® PDMS showed cracks, which under strain evolve in the regions of the defects, whereas the gold on SH-PDMS follows strains larger than 20%, without forming cracks. The peel-off tests represented in the photographs in Fig. 2(c) reveal that the Au/SH-PDMS on pure Sylgard® PDMS can be removed partially.

3.2 Au/SH-PDMS Films on Oxygen Plasma-Activated Sylgard® 184 PDMS

To improve the wetting of the SH-PDMS on Sylgard® PDMS, Sylgard® PDMS surface was exposed to oxygen plasma, using a power of 100 W for a period as short as 6 s. This parameter
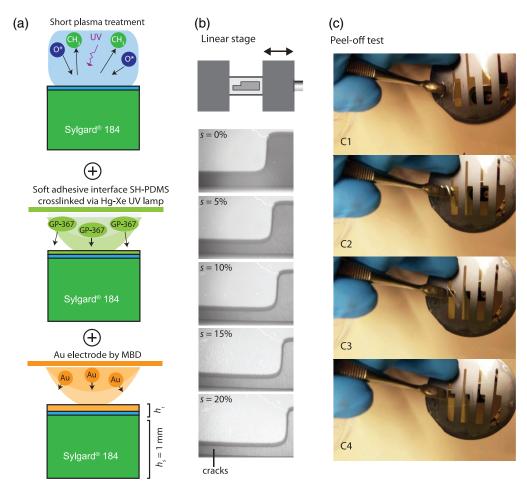

Fig. 2 The deposition of SH-PDMS (GP367) films on a native Sylgard® PDMS surface leads to characteristic defects, which might originate from repelling methyl–methyl groups before the UV cross linking is applied. (b) The one-dimensional stretching of the Au/SH-PDMS/Sylgard® PDMS is presented by a scheme and optical images. (c) The peel-off tests show that the Au/SH-PDMS has been partially removed.

choice resulted in a silica-like film on the Sylgard® PDMS. The mild plasma treatment did not induce enough compressive stress to cause wrinkle formation. Subsequent to plasma activation, the SH-PDMS film was grown and UV-cured for a period of 10 min, following which the gold was deposited. These layered Au/SH-PDMS structures adhered correctly onto the plasma-activated Sylgard® PDMS surface. Figure 3(c) shows such a pull-off test.

Au/SH-PDMS electrodes prepared on the activated Sylgard® PDMS, as outlined above, can be linearly strained with no visual structural changes, cf. Fig. 3(b). Nevertheless, strains larger than 5% cause cracks in the nanometer-thin and brittle SiO_x layer generated by the mild plasma treatment. Thus, one should try to reduce the power for the oxygen plasma treatment or activate the surface using UV irradiation.
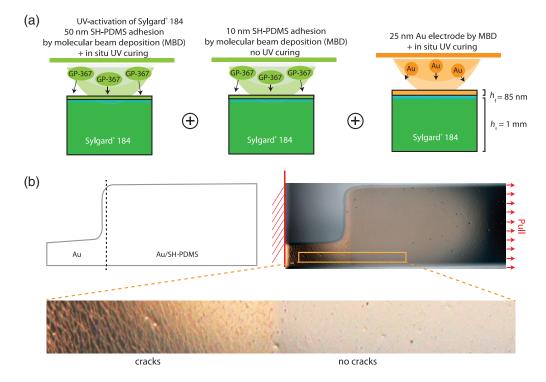
3.3 Molecular Beam Deposition of Au/SH-PDMS on UV-Activated Sylgard® PDMS

It has been reported recently that UV curing of Au/SH-PDMS can be performed effectively during and after the deposition of Au on SH-PDMS.[24] Simultaneously, the applied UV radiation can serve to activate moderately the underlying Sylgard® PDMS, as shown in Fig. 4. Exemplarily, *in situ* UV-curing was applied at the same time as the 50-nm-thin SH-PDMS layer was grown. Here, molecular beam deposition is not solely an additive manufacturing method, as specific interfaces of deeper structures can be treated and processed intentionally.

Fig. 3 (a) Au/SH-PDMS on plasma-treated Sylgard® PDMS. Oxygen plasma treatment results in an improved wetting of the Sylgard® PDMS surface. (b) Applying reasonable strains, cracks in the SiO_x layer below SH-PDMS become visible. (c) Peel-off tests show that the Au/SH-PDMS layer can adhere well to the stretchable PDMS substrate.
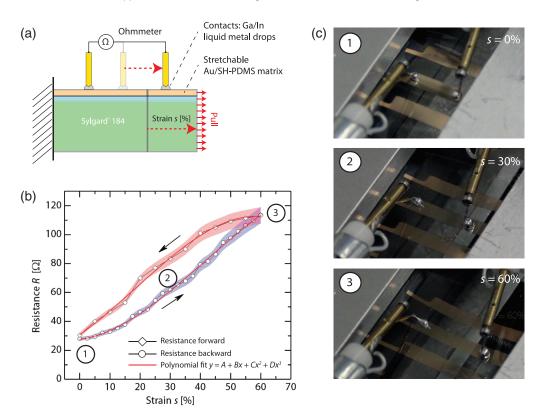
Fig. 4 (a) Scheme of the procedure employed to build a highly stretchable nanometer-thin electrode exploiting molecular beam deposition of SH-PDMS with UV irradiation during the deposition, followed by SH-PDMS deposition without UV treatment and gold deposition with UV irradiation. The Sylgard® PDMS was first UV-treated, to ensure the necessary wetting for the SH-PDMS layer. (b) Such Au/SH-PDMS electrodes survive strains of at least 60%. Contrary to Au/PDMS, which form numerous cracks, the incorporated thiol bonds prevent crack formation in the nanometer-thin layers.

A visual inspection of the obtained optical micrographs demonstrates that the SH-PDMS forms a uniform layer on the entire Sylgard® PDMS substrate. Obviously, on arrival, PDMS chains hitting the surface bind chemically to the growing film. In a next step, we deposited a 10-nm-thin SH-PDMS layer, without applying UV irradiation. Onto these unlinked SH-PDMS polymer chains, 25-nm Au was deposited thermally and formed covalent bonds with the thiol groups to the PDMS chains, which we cross linked afterward via UV irradiation. Such Au/SH-PDMS nanostructures can be regarded as compliant layers as we were unable to observe cracks or delamination, even when applying strains as large as 60%.

3.4 Electrical Conductivity of the Au/SH-PDMS Nanostructures

Using the simple two-wire method, resistance of Au/SH-PDMS electrodes as a function of the applied strain was measured, as shown in Fig. 5. For this purpose, liquid metal drops were placed on the Au/SH-PDMS nanostructures with the aim of guaranteeing low-resistance contacts (<1 Ω). Before the 4-mm-wide nanostructure was stretched linearly, the resistance along the 10-mm-long stripe was found to be (28 ± 2) Ω, which then increased to (62 ± 3) Ω at 30% strain and to (114 ± 5) Ω at 60% strain. The relaxation curve shows hysteresis. For example, the resistance at 30% strain is about 22 Ω higher compared with the forward approach. As there was no exponential increase in resistance, one can reasonably assume that at strains even higher than 60% the nanostructure remains conductive. Note that the experimental setup limited the maximal applicable strain to 60%.

Resistance $R = \rho L / W h_f$ is a function of resistivity ρ, the distance between liquid metal contacts L, width W, and thickness h_f. The measurement provided resistance R as a function of strain s. The experimental data were fitted with a third-order polynomial $R(s) = A + Bs + Cs^2 + Ds^3$. Increasing the strain, we obtained $A = (27.6 \pm 0.5)$ Ω, $B = (0.25 \pm 0.1)$ Ω per
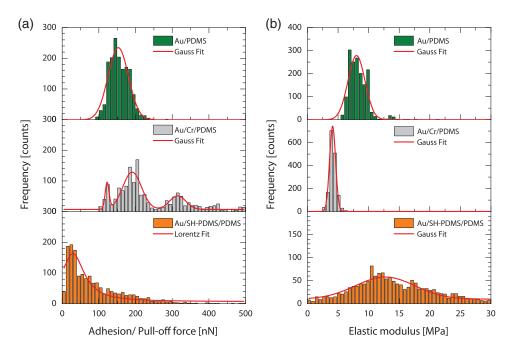
Fig. 5 Nanometer-thin Au/SH-PDMS electrodes remain conductive for strains up to 60%. (a) Scheme of the experimental setup, (b) Resistance-strain dependence, and (c) Photographs show the experimental setup at selected strain values. The liquid metal drops were fixed at the two parts of the linear stage, i.e., one contact was moved with respect to the other one.

1% strain, $C = (0.04 \pm 0.005)$ Ω per (1% strain)^2, and $D = -(0.0003 \pm 0.00005)$ Ω per (1% strain)^3. For strains of 60%, the fit was dominated by the linear contribution. Decreasing the strain, we derived the fitting parameters $A = (30.8 \pm 0.9)$ Ω, $B = (1.5 \pm 0.2)$ Ω per 1% strain, $C = (0.02 \pm 0.001)$ Ω per (1% strain)^2, and $D = -(0.0004 \pm 0.0001)$ Ω per (1% strain)^3. Here, the linear term also dominated. Therefore, one could conclude that as a first approximation, $R(s) = A + Bs$ is a valid description. For $R = 28$ Ω, $L = 10$ mm, $W = 4$ mm, and $h_f = 85$ nm, the resistivity $\rho = 9.6 \times 10^{-7}$ Ωm was only a factor of 40 lower than for bulk Au at a temperature of 20°C. Assuming that the Au/SH-PDMS electrode is incompressible, one finds for $R = 114$ Ω, $L = 16$ mm, $W = 4$ mm, and $h_f = 51$ nm a resistivity $\rho = 1.4 \times 10^{-6}$ Ωm. This means that resistivity ρ increased by 50% when stretching the nanostructure by 60%. These preliminary data, however, have to be taken with care because of the crude experimental approach. A foreseen four-point measurement will yield precise resistivity data.

3.5 Mechanical Properties Derived from Atomic Force Microscopy Nanoindentation Measurements

The set of 1600 force–distance curves allowed us not only to extract the mechanical properties of the compliant electrodes, but also to study the related adhesion forces. Figure 6(a) shows the adhesion/pull-off forces of the AFM cantilever with a CH$_3$-functionalized Au bead and the Au electrode. The experimental data were fitted by means of Gaussians or Lorentzians. For thermally evaporated gold on the nontreated PDMS substrates, we found a mean value of (150 ± 55) nN. For the Au/Cr electrodes, three peaks with maxima at (123 ± 5), (190 ± 25), and (315 ± 23) nN were present. The three peaks could be related to the wrinkled surface, which is brought into contact with the spherical indenter with a diameter of 2 μm. Note that the diameter of the spherical bead is close to the wrinkle periodicity of (1.9 ± 0.1) μm of the Au/Cr electrode, cf. Fig. 1(b). The obtained adhesion forces related to the contact area of the indenter,

Fig. 6 Histograms of pull-off forces and elastic moduli extracted from force–distance curves for a CH_3-functionalized AFM tip and the conductive Au layer. (a) Unloading curves from the nano-indentation experiments include pull-off forces. AFM tips with a spherical bead 2 μm in diameter were used. For the Au/SH-PDMS, the relatively small pull-off forces relate to repulsive forces between the CH_3-groups on the bead and in the SH-PDMS network. (b) The elastic modulus of (12 ± 9) MPa for the Au/SH-PDMS electrode is higher than expected, probably due to UV irradiation lasting 1 h. Reducing the irradiation time, one may reduce the elastic modulus substantially.

given by its radius.[31] Therefore, the peak with the highest adhesion force is associated with the groove-like depressions, whereas the peak with the lowest adhesion force corresponds to the protrusions of the wrinkled surface.

Au/SH-PDMS electrodes showed adhesion forces of a few 10 nN. We interpret such small values as the repulsive interactions between the CH_3-groups of the indenter bead and the SH-PDMS network. In addition, higher adhesion forces of up to 300 nN were found, which might originate from clusters of pure Au. This observation indicates that Au clusters are incorporated into the SH-PDMS network. The gold does not simply cover the surface of the SH-PDMS, as found for Au on nontreated PDMS.

The elastic moduli are calculated from 1600 NI, using the JKR contact model, which accounts for the adhesion forces. Figure 6(b) shows the derived experimental data, fitted by means of a Gaussian. We found elastic moduli of (8 ± 3), (4.1 ± 0.5), and (13 ± 10) MPa for Au/PDMS, Au/Cr/PDMS, and Au/SH-PDMS/PDMS, respectively.

The elastic modulus of the Au/SH-PDMS/PDMS is high in comparison with the pure Au on PDMS. We must note here that the UV irradiation dose during the deposition of the 50-nm-thin adhesion layer has not been optimized yet. It has been shown that the elastic modulus increases in line with dose for a given deposition rate.[32] As a consequence, we are convinced that a lower UV irradiation dose than used in the present study will result in much softer Au/SH-PDMS electrodes.

4 Conclusions

In the present study, we developed a procedure to realize highly compliant electrodes for DETs. Elastomer films tens of nanometers thin, along with subsequently deposited Au, form a highly compliant Au/SH-PDMS conductor with a total thickness of <85 nm. The gold and the thiol groups form covalent bonds. This bonding prevents the diffusion of gold into the underlying layers. Uniaxial stretch tests demonstrate that Au/SH-PDMS layers do not form cracks and

remain highly conductive for strains of at least up to 60%. From the pull-off forces derived from nanoindentation experiments with a CH_3-functionalized AFM tip, we conclude that the Au is not a film but its clusters are indeed incorporated into the nanometer-thin SH-PDMS layer. Such nanometer-thin, soft, highly compliant, and conductive layers will enable us to realize multilayer, low-voltage dielectric transducers.

Acknowledgments

References

1. Y. Bar-Cohen, *Electroactive Polymer (EAP) Actuators as Artificial Muscles: Reality, Potential, and Challenges*, SPIE Press, Bellingham, Washington (2004).
2. P. Brochu and Q. Pei, "Advances in dielectric elastomers for actuators and artificial muscles," *Macromol. Rapid. Commun.* **31**, 10–36 (2010).
3. I. A. Anderson et al., "Multi-functional dielectric elastomer artificial muscles for soft and smart machines," *J. Appl. Phys.* **112**, 041101 (2012).
4. F. Carpi et al., "Standards for dielectric elastomer transducers," *Smart Mater. Struct.* **24**, 105025 (2015).
5. A. Poulin, S. Rosset, and H. Shea, "Fully printed 3 microns thick dielectric elastomer actuator," *Proc. SPIE* **9798**, 97980L (2016).
6. S. Rosset and H. Shea, "Small, fast, and tough: Shrinking down integrated elastomer transducers," *Appl. Phys. Rev.* **3**, 031105 (2016).
7. F. Carpi et al., *Dielectric Elastomers as Electromechanical Transducers*, Elsevier, Amsterdam (2011).
8. M. Duduta, R. J. Wood, and D. R. Clarke, "Multilayer dielectric elastomers for fast, programmable actuation without prestretch," *Adv. Mater.* **28**, 8058–8063 (2016).
9. T. Töpper et al., "Siloxane-based thin films for biomimetic low-voltage dielectric actuators," *Sens. Actuators, A* **233**, 32–41 (2015).
10. B. Osmani, E. A. Aeby, and B. Müller, "Stress measurements of planar dielectric elastomer actuators," *Rev. Sci. Instrum.* **87**, 053901 (2016).
11. E. Fattorini et al., "Artificial muscle devices: innovations and prospects for fecal incontinence treatment," *Ann. Biomed. Eng.* **44**, 1355–1369 (2016).
12. T. Töpper et al., "Leakage current, self-clearing and actuation efficiency of nanometer-thin, low-voltage dielectric elastomer transducers tailored by thermal evaporation," *Proc. SPIE* **10163**, 101631F (2017).
13. H. Schmid et al., "Preparation of metallic films on elastomeric stamps and their application for contact processing and contact printing," *Adv. Funct. Mater.* **13**, 145–153 (2003).
14. B. Osmani et al., "Micro- and nanostructured electro-active polymer actuators as smart muscles for incontinence treatment," *AIP Conf. Proc.* **1646**, 91–100 (2015).
15. B. Osmani et al., "Gold layers on elastomers near the critical stress regime," *Adv. Mater. Technol.* **2**, 1700105 (2017).
16. S. P. Lacour, G. Courtine, and J. Guck, "Materials and technologies for soft implantable neuroprostheses," *Nat. Rev. Mater.* **1**, 16063 (2016).

17. T. Li et al., "Stretchability of thin metal films on elastomer substrates," *Appl. Phys. Lett.* **85**, 3435–3437 (2004).
18. Y.-L. Loo et al., "Additive, nanoscale patterning of metal films with a stamp and a surface chemistry mediated transfer process: applications in plastic electronics," *Appl. Phys. Lett.* **81**, 562–564 (2002).
19. I. Byun, A. W. Coleman, and B. Kim, "Transfer of thin Au films to polydimethylsiloxane (PDMS) with reliable bonding using (3-mercaptopropyl) trimethoxysilane (MPTMS) as a molecular adhesive," *J. Micromech. Microeng.* **23**, 085016 (2013).
20. K. Efimenko, W. E. Wallace, and J. Genzer, "Surface modification of Sylgard-184 poly (dimethyl siloxane) networks by ultraviolet and ultraviolet/ozone treatment," *J. Colloid. Interface Sci.* **254**, 306–315 (2002).
21. W. Kaczorowski et al., "Effect of plasma treatment on the surface properties of polydimethylsiloxane," *J. Appl. Polym. Sci.* **132**, 41635 (2015).
22. B. Osmani et al., "Morphology and conductivity of Au electrodes on polydimethylsiloxane using (3-mercaptopropyl) trimethoxysilane (MPTMS) as an adhesion promoter," *Proc. SPIE* **9798**, 979822 (2016).
23. H. Grönbeck, A. Curioni, and W. Andreoni, "Thiols and disulfides on the Au (111) surface: the headgroup-gold interaction," *J. Am. Chem. Soc.* **122**, 3839–3842 (2000).
24. T. Töpper et al., "Time-resolved plasmonics on self-assembled hetero-nanostructures for soft nanophotonic and electronic devices," *Adv. Electron. Mater.* **3**, 1700073 (2017).
25. A. Chandekar, S. K. Sengupta, and J. E. Whitten, "Thermal stability of thiol and silane monolayers: a comparative study," *Appl. Surf. Sci.* **256**, 2742–2749 (2010).
26. C. Dölle et al., "Gradual photochemical-induced conversion of liquid polydimethylsiloxane layers to carbon containing silica coatings by UV irradiation at 172 nm," *Langmuir* **25**, 7129–7134 (2009).
27. L. Prager et al., "Vacuum-UV Irradiation-Based Formation of Methyl-Si-O-Si Networks from Poly(1, 1-Dimethylsilazane-co-1-methylsilazane)," *Chem. Eur. J.* **15**, 675–683 (2009).
28. E. S. John, W. M. C. James, and M. Paul, "Calibration of rectangular atomic force microscope cantilevers," *Rev. Sci. Instrum.* **70**, 3967–3969 (1999).
29. S. Gupta et al., "Adhesive forces significantly affect elastic modulus determination of soft polymeric materials in nanoindentation," *Mater. Lett.* **61**, 448–451 (2007).
30. O. Graudejus, P. Görrn, and S. Wagner, "Controlling the morphology of gold films on poly (dimethylsiloxane)," *ACS Appl. Mater. Interfaces* **2**, 1927–1933 (2010).
31. B. Osmani et al., "Nanomechanical probing of thin-film dielectric elastomer transducers," *Appl. Phys. Lett.* **111**, 093104 (2017).
32. T. Töpper, B. Osmani, and B. Müller, "Polydimethylsiloxane films engineered for smart nanostructures," *Microelectron. Eng.* **194**, 1–7 (2018).

Bekim Osmani received his MSc degree in biomedical engineering from the ETH Zurich for work on contractile cell force measurements using cantilevers in 2002. After working more than 10 years in academia and industry, he performed a PhD thesis in the field of nanosciences at the University of Basel on nanostructured dielectric elastomer transducers for smart implants. Currently, he is a research associate at the medical faculty and deals with nanotechnology-based implants for various patient treatments.

Tino Töpper received his MSc degree in physics from the University in Freiburg, Germany, in 2012. He received his PhD in physics from the University of Basel on spectroscopic ellipsometry on tailored siloxane-based nanostructures for low-voltage dielectric elastomer actuators in 2016. Currently, he is a research associate at the medical faculty and heads the Bridge project "Enhancing the capabilities of artificial muscle implants using low-voltage dielectric elastomer sensors."

Bert Müller holds the Thomas Straumann chair of materials science in medicine at the University of Basel. His current research interests include high-resolution hard X-ray imaging, mechanoresponsive liposomes for targeted drug delivery, and artificial muscles. He has been elected as a fellow of SPIE and an active member of the European Academy of Sciences and Arts. Since 2001, he has been teaching at the physics department of ETH Zurich.